| Journal of Coastal Research | SI 39 | 556 - 560 | ICS 2004 (Proceedings) | Brazil | ISSN 0749-0208 |
|---|---|---|---|---|---|

# Fine Sediment Accumulation in a Harbor Protected by a Breakwater of Surface-Piercing Type

**J. L. Lee† and M. R. Oh‡**

†Dept. of Civil and Environmental Engineering
Sungkyunkwan University Suwon,
440-746, Korea
jllee6359@hanmail.net

‡ Dept. of Civil and Environmental Engineering
Sungkyunkwan University,
Suwon 440-746, Korea
namu387@skku.edu

**ABSTRACT**

LEE, J. L. and OH, M. R., 2006. Fine sediment accumulation in a harbor protected by a breakwater of surface-piercing type. Journal of Coastal Research, SI 39 (Proceendigs of the 8th International Coastal Symposium), 556 - 560. Itajaí, SC, Brazil, ISSN 0749-0208.

A surface-piercing barrier model is presented for understanding morphological development in the sheltered region and investigating the main factors causing the severe accumulation. Surface-piercing structures like vertical barriers, surface docks and floating breakwaters are recently favored from the point of view of a marine scenario since they do not in general partition the natural sea. The numerical solutions are compared with experimental data on wave profiles and morphological change rates within a rectangular harbor of a constant depth protected by surface-piercing thin breakwaters as a simplified problem. Our numerical study involves several modules: 1) wave dynamics analyzed by a plane-wave approximation, 2) suspended sediment transport combined with sediment erosion-deposition model, and 3) concurrent morphological changes. Scattering waves are solved by using a plane wave method without inclusion of evanescent modes. Evanescent modes are only considered in predicting the reflection ratio against the vertical barrier and energy losses due to vortex shedding from the lower edge of plate are taken into account. A new relationship to relate the near-bed concentration to the depth-mean concentration is presented by analyzing the vertical structure of concentration. The numerical solutions were also compared with experimental data on morphological changes within a rectangular harbor of constant water depth. Through the numerical experiments, the vortex-induced flow appears to be not ignorable in predicting the morphological changes although the immersion depth of a plate is not deep.

**ADDITIONAL INDEX WORDS:** *Scattering wave, mild-slope equation, energy loss, sediment deposition rate, morphological change.*

## INTRODUCTION

The breakwater of surface-piercing type has been developed mainly for application within bays or estuaries that are semi-protected from the direct impact of large waves. Most of bays have soft foundation which is too weak to bear the weight of gravity type breakwater. Thus the surface-piercing barrier is taken into account as an alternative tool to reduce wave heights in the bay to an acceptable level. Differently from the ordinary breakwater of gravity type, the surface barrier reduces the transmitted waves mainly due to the reflection of incident waves from the barrier body. Traditional breakwaters, seawalls and jetties reflect or direct wave energy in destructive ways or concentrate it in local hot spots so that the concentrated energy leads to the destruction of marine facilities. Among a number of breakwaters, the vertical barriers with gaps are recently favored from the point of view of marine environment since they do not in general partition the natural sea.

The scattering of water waves by such structures has been solved previously by a number of authors but well known for the mathematical difficulties encountered within the framework of linearized potential theory. Therefore, vertical barrier performance by theoretical evaluations has been typically accomplished in the two-dimensional domain, in which the wave transmission and reflection characteristics are only taken into account. In harbors and marinas, however, incoming waves may be significantly diffracted and radiated beyond such structures and consequently reflected by harbor wharves and returned to them. Under such circumstances, it is essential for the wave-induced motion in a harbor to be solved numerically with taking into account the effect of wave deformation in a harbor.

The numerical approaches of the wave-structure interaction have concerned several authors. SAWARAGI *et al.* (1987) proposed a numerical method combining a three-dimensional Green's function model for near-field waves around a floating body and a two-dimensional BIEM model for far-field waves. Recently, OHYAMA and TSUCHIDA (1997) expanded the mild-slope equation incorporating evanescent modes to get much higher computational efficiency as compared to previous approaches. However, their new sets of mild-slope equations for evanescent modes still require significant CPU time and computational storage. As more simple approach for vertical barriers, LEE and LEE (2001) and LEE and LEE (2003) proposed a plane wave method to add scattering terms to the traditional mild-slope equation without inclusion of evanescent modes. The scattering term, which generates the scattering waves, is determined by the gradient of surface velocity potential across the barrier. Evanescent modes are only considered in predicting the reflection ratio against the vertical barrier.

There are a multitude of problems related to the transport of fine sediments and the absorbed pollutants along the west and south coast of Korea, which is abundant in fine-grained sediments. Harbors and navigation channels in such areas are affected by the severe accumulation of muddy sediments which makes dredging operations expensive and, if heavily polluted, requires additional disposal expenses of dredged material. Although studies on the sediment transport have started due to an increasing demand for harbors, the morphological development in a harbor is still poorly understood.

In the present study, a surface-piercing barrier model is presented to understand morphological development in the sheltered region and investigates the main factors causing the severe accumulation. The effects of bed load transports are ignored in this study as a preliminary study.

## HYDRODYNAMICS

### Governing Equation

The time dependent mild-slope equations are given below, in which the wave generating and scattering terms are inserted (LEE and LEE, 2003).

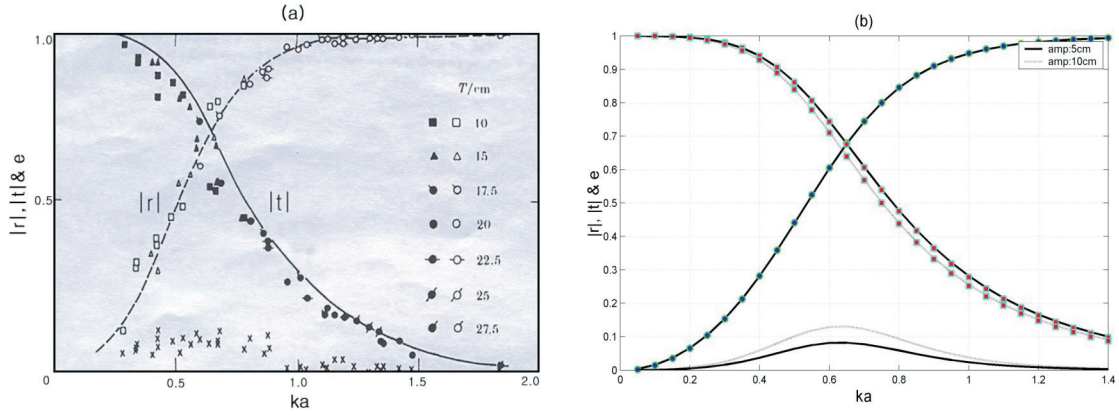


Figure 1. Performance test; (a) STIASSNIE *et al.* (1984)'s measurements and (b) numerical results for a vertical barrier (lines : analytical solutions, symbols : model results).

$$\frac{\partial^2 S}{\partial t^2} + 2i\sigma\frac{\partial S}{\partial t} + \nabla\left[\frac{CC_g}{g}\left(\frac{\partial \mathbf{U}}{\partial t} + i\sigma\,\mathbf{U}\right)\right] - k^2 CC_g S = S_i \qquad (1)$$

$$\frac{\partial \mathbf{U}}{\partial t} + i\sigma\,\mathbf{U} + g\nabla S = \mathbf{U}_s \qquad (2)$$

where $S_i$ is the source term which generates the incoming waves and $U_s$ is the scattering term . The source term is given in terms of the incident wave height $H_i$ and the scattering term in terms of $\mathbf{U}$ on the grid mesh of $\Delta x$ and $\Delta y$:

$$S_i = \frac{\sigma C_g H_i}{\Delta x} \qquad (3)$$

$$\mathbf{U}_s = 2C\frac{r}{t}\frac{\mathbf{U}}{\Delta x} \qquad (4)$$

Where, $r$ is the reflection coefficient, and $t$ is the transmission coefficient.

The governing equations (1) and (2) are solved by the approximate factorization techniques leading to the implicit finite difference schemes. The scheme is applied with the complex variables defined on a space-staggered rectangular grid. The more detailed description is given in LEE and LEE (2003).

## Energy Dissipation

In nature, the presence of the obstacle may induce vortex breakdown, which in turn introduces vorticity in the flow. The most important consequence of vorticity production is energy dissipation at the expense of the transmitted waves. So now we consider the waves whose energy is dissipated.

Energy losses due to vortex shedding from the lower edge of a vertical plate attacked by surface waves. The energy dissipation coefficient, which is determined as the ratio between the flux of the energy taken out by the vortex generation process, and the incoming wave energy flux, is given by (STIASSNIE *et al.*, 1984) as

$$e = \frac{D(ka_o)^{(2/3)}}{ka[K_1^2(ka) + \pi^2 I_1^2(ka)]^2} \qquad (5)$$

The above formula is only valid for deep water waves but is applicable for the immersion depth relatively low to water depth.

Using Eq. (5), we can obtain $r/t$ which can be given as

$$\frac{r}{t} = \frac{e/2 - i\sqrt{(|r_o|^2 + \varepsilon)(|t_o|^2 - \varepsilon) - e/2}}{|t_o|^2 - \varepsilon - e/2} \qquad (6)$$

where $a_0$ and $k$ are the amplitude and wave number of the incoming wave, respectively and a is the draught of the plate. $r_0$ and $t_0$ are determined under no dissipation. $e$=0 implies that the energy dissipation equally assigned to reflection and transmission coefficients, while $e$=ε/2 implies that all energy dissipation occurs when waves transmit. Figure 1 shows the model performance of wave reflection and transmission for energy dissipation calculated by Eq (5). The model was run for two amplitudes of 5 and 10cm, respectively, to examine the effect of wave amplitude.

## Comparison with Measured Wave Profiles

A harbor model with surface-piercing breakwaters was set in a Sungkyunkwan University wave flume consisted of a wave generator and absorber. The regular waves were generated by the piston-type wave paddle. The flume is 12m long, 0.4m wide and 0.5m deep with the still water depth being maintained at 0.2m.

The whole length of a harbor is 1.5m, the end of harbor is closed by an impermeable wall and the harbor is protected by two barriers whose spacing is 0.462m as shown in Fig. 3. The water depth in the harbor is 0.18m due to the bed level.

The bottom and sides walls of the flume are glass to allow easy optical access. As shown in Figure 2, the wave flume was decorated with the data acquisition system accessing the wave profile signals from the gages. Physical experiments were accomplished for two different wave periods as given in Table 1. The incident wave heights were measured only with a wave absorbor of the other end without a harbor model.

The layout of experimental configuration is illustrated in Figure 2, showing the locations of the measurement stations and detailed geometry of the flume. The model calculation was performed on the grid mesh of 290x52 and grid size of 8mm. Figure 3 shows the comparison between the numerical results and measured wave profiles. With inclusion of energy dissipation, the good agreement was obtained. STIASSNIE *et al.* (1984) suggested 2.16 as $D$ value in Eq. (4), however, the better results was obtained with $D$ of 4. For case 1, the dissipation effects are relatively small.

# MORPHODYNAMICS

## Depth-Averaged Model

The rates of sea bed change mainly due to the suspended sediment transport can be predicted by

Table 1. *Experimental conditions.*

| | Period | $H_i$ | a/h | r | e |
|---|---|---|---|---|---|
| Case 1 | 0.80s | 3.9 cm | 0.21 | 0.073 | 0.178 |
| Case 2 | 0.69s | 5.5 cm | 0.21 | 0.112 | 0.352 |

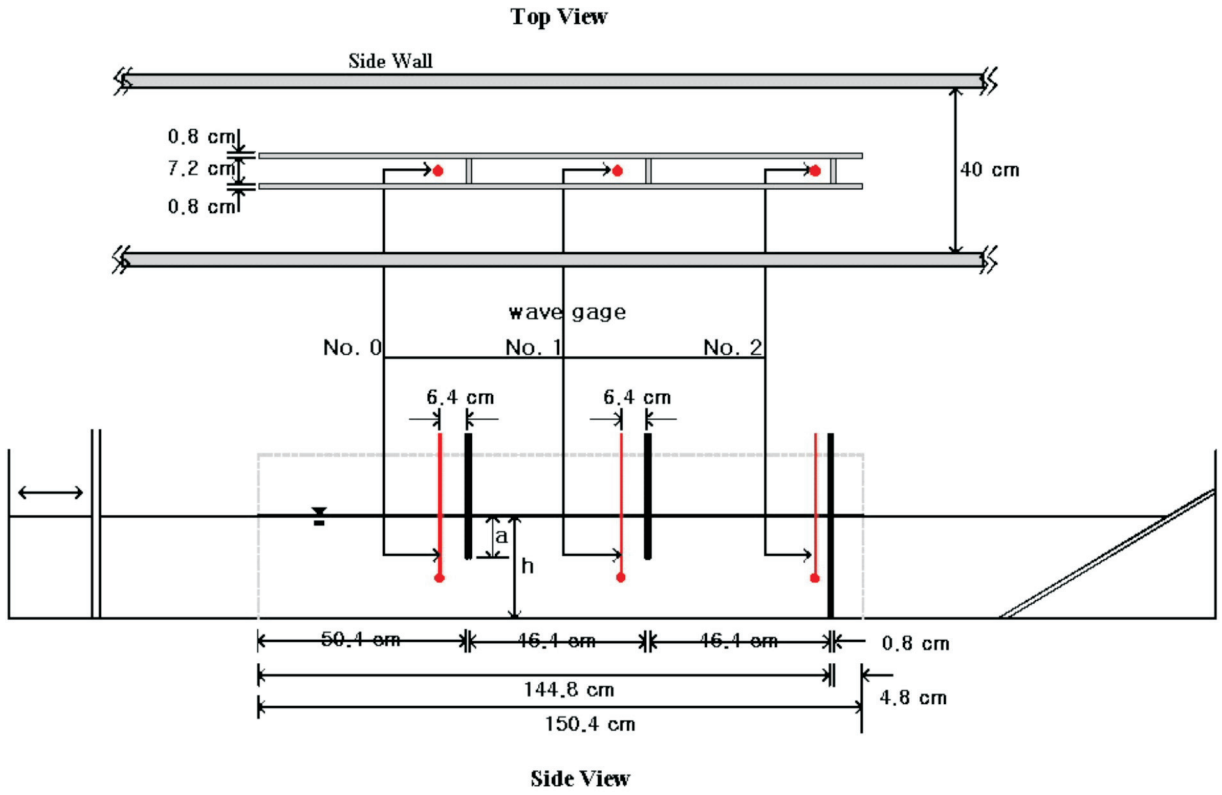


Figure 2. Physical layout of experiment.

$$\frac{dh}{dt} = S_E - S_D \tag{7}$$

where $H$ is the water depth to the active sea bed, $S_D$ is the rate of bed deposition and $S_E$ is the rate of bed erosion.

Since $S_D$ is estimated by the concentration of suspended sediments, the advective-dispersive equation of suspended sediments has to be solved:

$$\frac{\partial C}{\partial t} + u\frac{\partial C}{\partial x} + v\frac{\partial C}{\partial y} + (w - w_f)\frac{\partial C}{\partial z} = K_h\left[\frac{\partial^2 C}{\partial x^2} + \frac{\partial^2 C}{\partial y^2}\right] + K_z\frac{\partial^2 C}{\partial z^2} \tag{8}$$

Where, $C$ is the volume replaced by sediments per unit sea water volume as a normalized concentration, $w_f$ the net sedimentation rate constant, $K_H$ is the horizontal diffusion coefficient, *and* $K_z$ is the vertical diffusion coefficient. Taking depth-integration, we can obtain

$$\frac{\partial C}{\partial t} + u\frac{\partial C}{\partial x} + v\frac{\partial C}{\partial y} = K_h\left[\frac{\partial^2 C}{\partial x^2} + \frac{\partial^2 C}{\partial y^2}\right] - \frac{S_D - S_E}{h} \tag{9}$$

Where, $S_D = w_f C_b(1-\tau/\tau_{CD})$ the rate of bed deposition, $\tau_{CD}$ the critical bed shear stress that prevents deposition, $C_b$ the concentration near the bottom, $SE = M(\tau-\tau_{CE})$ the rate of bed erosion, $M$ the erodibility coefficient, $\tau_{CE}$ the critical bed shear required for resuspension. The critical shear stresses mentioned above are not included in the present numerical simulation. The velocity components employed in Eq. (9) are near-bottom particle velocities which are modified using the eigenfunction expansion method to include evanescent modes.

We now present the $C_b$ in terms of the vertical process variables of sediments, $w_f$ and $K_z$. Under the same hydrodynamic and sediment conditions in space and the steady state condition in time, Eq. (8) can be written as

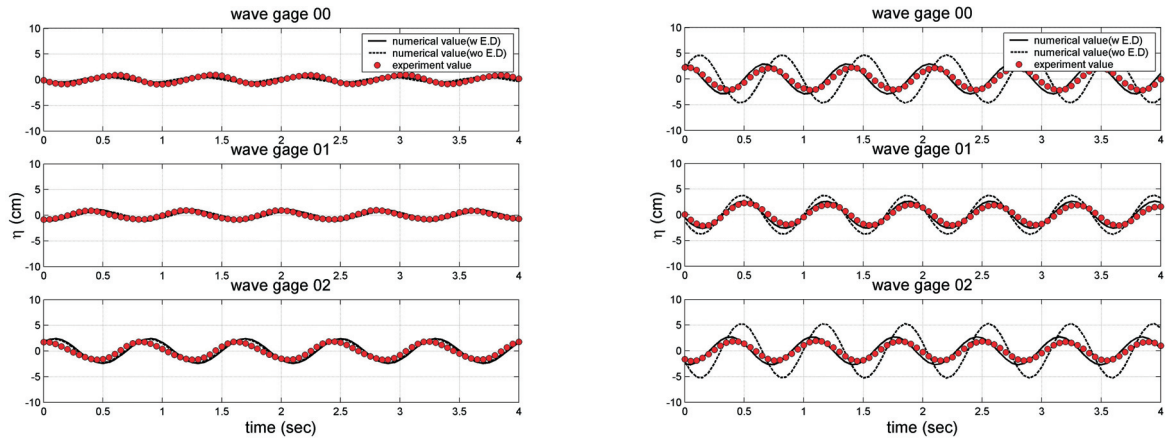


Figure 3. Comparison with measured wave profiles for (a) period 0.8sec and (b) for period 0.69sec (solid line: with losses, dashed line: without losses).

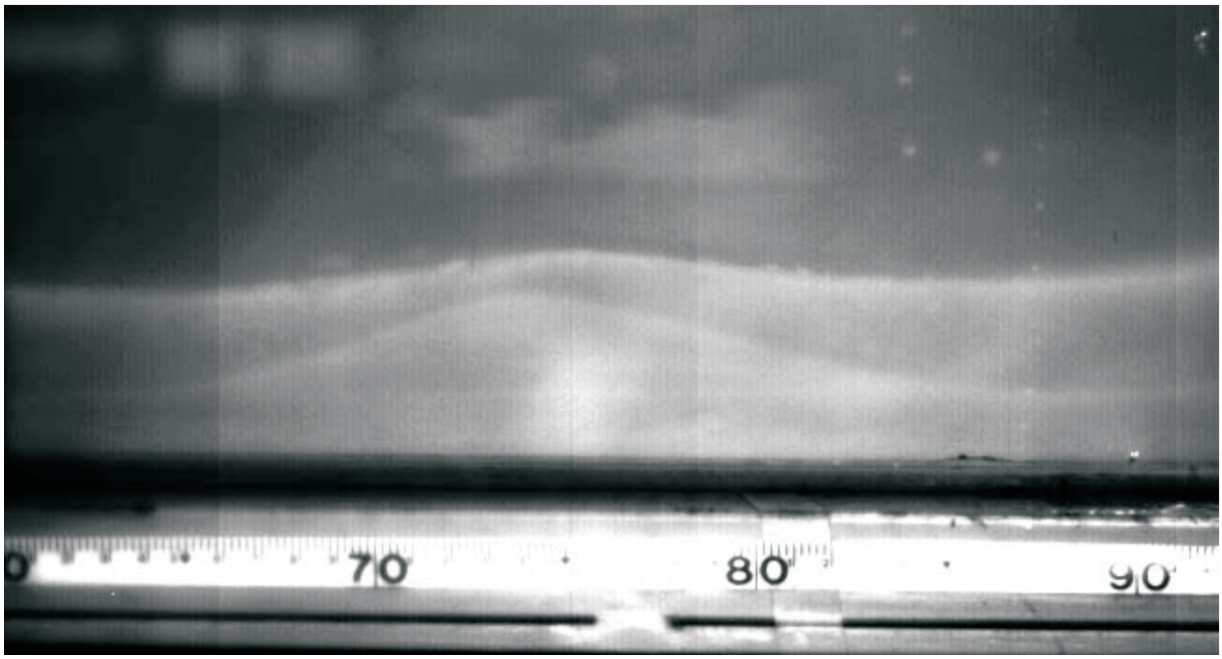


Figure 4. Two layers of sediments formed under wave action.

$$K_z \frac{\partial^2 C}{\partial z^2} + w_f \frac{\partial C}{\partial z} = 0 \qquad (10)$$

Which yields

$$C = \frac{w_f h}{K_z} C \quad \text{for} \quad \frac{w_f h}{K_z} >> 1 \qquad (11)$$

under the assumption that the surface concentration is nearly zero. It is noticeable that the rapid deposition process is observed as a dimensionless parameter $w_f h/K_z$ increases.

The suspended sediment transport is determined by a new hybrid method which is superior in both result accuracy and time-saving ability. It is based on the forward-tracking particle method for advection. However, unlike the conventional random-walking method, it solves the diffusion process on the fixed Eulerian grids, which requires neither an interpolating algorithm nor large number of particles.

## Comparison with Measured Bed Level Changes

A sediment layer of 2cm was laid with Milk Casein on the acryl bottom of a harbor model. The sill of 2cm was put on the side of a harbor entrance to keep the sediments from sliding out.

The mean grain size, specific gravity and settling velocity of Milk Casein used were measured to be 0.24mm, 1.41 and 6.4mm/s, respectively.

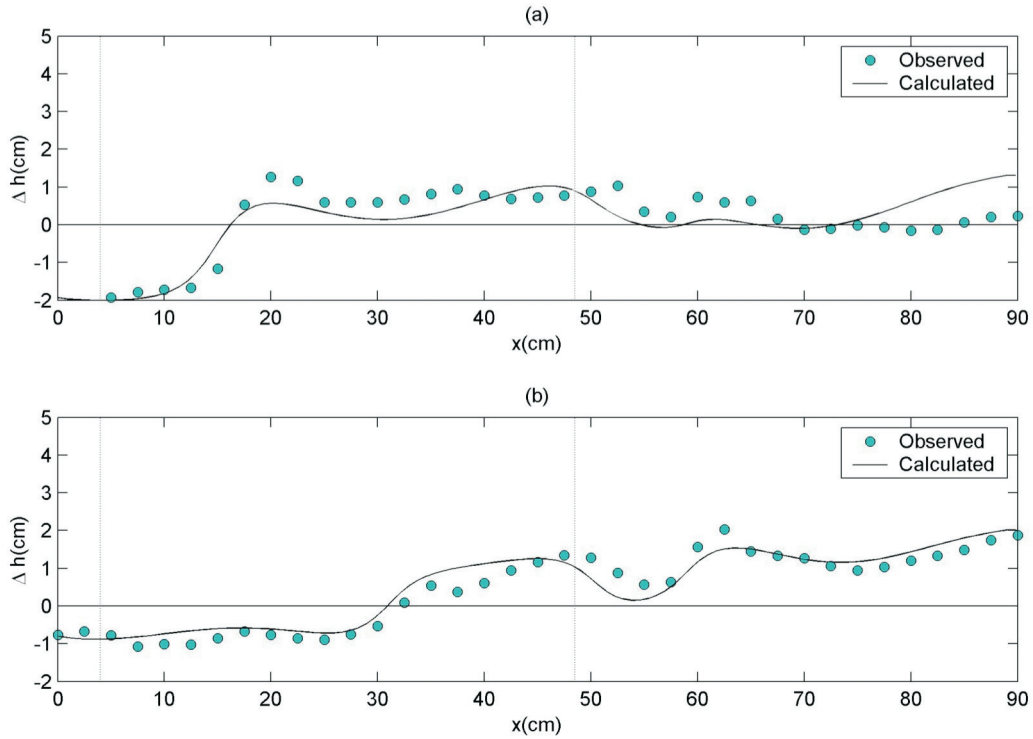


Figure 5. Comparison with measured bottom bed levels after 5minutes for (a) period 0.8sec and (b) for period 0.69sec (dotted vertical lines: the barrier position).

The bed levels were extracted from the images taken by a CCD camera. Two layers were observed under wave action as shown in Figure 4. The surface of top layer, which shows the better mass conservation, was compared with numerical results. Experiments on bed level changes were also accomplished for two different wave conditions as given in Table 1.

In both the cases shown in Figure 5, numerical results show good agreement with laboratory data with use of $M$ = 2s/m, $K_h$ =1m$^2$/s and $K_z/w_f$ = 0.05m. Thus the erodibility coefficient of Milk Casein is estimated to be very large when compared with regular sand sediments. It may be caused by its low specific gravity. In the figure, the vertical wall is located at $x$=95.5cm.

The bed profiles were measured after 5 minutes from the initially flat bottom. Measured data indicate that bed material is eroded from the higher wave energy zone and deposited on the lower energy zone. From numerical experiments, it is found that the vortex-induced flow plays an important role in predicting the morphological changes although the immersion depth of a plate is not deep. For the wave condition of 0.8sec, the acryl bottom on the left end in the figure was exposed after 5min.

## CONCLUSIONS

This paper describes a surface-piercing barrier model designed for understanding morphological development in the sheltered region and investigating the main factors causing the severe accumulation. The barrier of surface-piercing type has characteristics that control wave intrusion but allow the free sediment transport.

Scattering waves were approximately solved by extending the mild-slope equation. In addition, energy losses due to vortex shedding from the lower edge of plate were taken into account. The agreement with laboratory data is generally satisfactory with the inclusion of energy dissipation effects.

A new relationship is presented to relate the near-bed concentration to the depth-mean concentration analyzing the vertical structure of concentration. To evaluate unknown parameters on sediment processes, the numerical solutions were compared with experimental data on morphological changes within a rectangular harbor of a constant depth. The vortex-induced flow, which is formed behind the barrier, appears to be not ignorable in predicting the morphological changes although the immersion depth of a plate is not deep.

## ACKNOWLEDGEMENTS

This research was financially supported by the Korea Ministry of Marine Affairs and Fisheries.

## LITERATURE CITED

LEE, J.L. and LEE, K.J., 2001. Effect of a surface-piercing vertical thin breakwater to harbor tranquility. The First Asian and Pacific Coastal Engineering Conference, pp. 186-195.

LEE, J.L. and LEE, D.Y., 2003. Modeling of wave scattering by vertical barriers. Proc. of 13th International Offshore and Polar Engineering Conference, ISOPE, Vol. 3, pp. 773-780.

OHYAMA, T. and TSUCHIDA, M., 1997. Expanded mild-slope equations for the analysis of wave-induced ship motion in a harbor. Coastal Engineering 30, pp. 77-103.

SAWARAGI, T.; AOKI, S. and HAMAMOTO, S., 1989. Analysis of hydrodynamic forces due to waves acting on a ship in a harbor of arbitrary geometry. Proc. 8th Int. Conf. Offshore Mech. and Arctic Eng., ASME, pp. 117-123.

STIASSNIE, M.; NAHEER, E. and BOGUSLAVSKY, I., 1984. Energy losses due to vortex shedding from the lower edge of a vertical plate attacked by surface waves. Proc. R. Soc. Lond. A396, pp. 131-142.